PERGAMON

International Journal of Heat and Mass Transfer 45 (2002) 755–764

International Journal of HEAT and MASS TRANSFER

www.elsevier.com/locate/ijhmt

Heat transfer in a pulsating heat pipe with open end

Yuwen Zhang [1], Amir Faghri *

Department of Mechanical Engineering, University of Connecticut, 191 Auditorium Road, Storrs, CT 06269-3139, USA

Received 11 July 2000; received in revised form 6 June 2001

Abstract

Heat transfer in the evaporator and condenser sections of a pulsating heat pipe (PHP) with open end is modeled by analyzing thin film evaporation and condensation. The heat transfer solutions are applied to the thermal model of the pulsating heat pipe and a parametric study was performed. The results show that the heat transfer in a PHP is mainly due to the exchange of sensible heat. The frequency and amplitude of the oscillation is almost unaffected by surface tension after steady oscillation has been established. The amplitude of oscillation decreases with decreasing diameter. The amplitude of oscillation also decreases when the wall temperature of the heating section is decreased, but the frequency of oscillation is almost unchanged. © 2001 Published by Elsevier Science Ltd.

1. Introduction

The pulsating heat pipe (PHP) is a very effective heat transfer device [1]. It consists of a relatively long and thin sealed pipe containing both phases of the working fluid. The inner diameter of the pipe must be sufficiently small so that vapor bubbles can grow to vapor plugs in the tube. The PHP is made from a long capillary tube bent into many turns and the evaporator and condenser sections are located at these turns. Compared with the traditional heat pipe, the unique feature of PHPs is that there is no wick structure to return the condensate to the evaporator section, and therefore there is no counter current flow between the liquid and vapor.

Both experimental and analytical/numerical investigation on PHPs has been carried out by some researchers. The experimental investigations mainly focus on visualization of flow pattern and measurement of temperature and effective thermal conductivity. While most researchers suggest that slug flow is the dominate flow pattern, Lee et al. [2] reported that oscillation of bubbles caused by nucleate boiling and vapor oscillation, and departure of small bubbles are considered as the representative flow pattern at the evaporator and adiabatic section, respectively. Although the accuracy of the effective thermal conductivities is somewhat questionable, the available experimental data can provide some base for verification of the theoretical model.

Dobson and Harms [3] performed a lumped parameter analysis on oscillatory heat pipes. The mathematical model is given for a heat pipe with an open end, and they mentioned that it can be applied also to the heat pipe with a closed end. They assumed that the effect of surface tension is negligible. They also assumed that there is no heat transfer between the liquid and its surroundings. The heat transfer coefficients between heated pipe wall and the vapor was simply assumed.

Hosoda et al. [4] investigated propagation phenomena of vapor plugs in a meandering closed loop heat transport device (MCL-HTD). They observed a simple flow pattern, appearing at high liquid volume fractions. In such a condition, only two vapor plugs exist separately in adjacent turns, and one of them starts to shrink when the other starts to grow. A simplified numerical solution is also performed with several major assumptions including neglecting liquid film which may exist between the tube wall and a vapor plug. They also neglected the effect of surface tension. The heat transfer coefficients were estimated from an empirical equation for convective flow.

* Corresponding author. Tel.: +001-860-486-2221; fax: +001-860-486-0318.

E-mail address: faghri@engr.uconn.edu (A. Faghri).

[1] Present address: Department of Mechanical Engineering, New Mexico State University, Las Cruces, NM 88003, USA.

0017-9310/02/$ - see front matter © 2001 Published by Elsevier Science Ltd.
PII: S0017-9310(01)00203-4

Nomenclature

c_p	specific heat at constant pressure (J/kg K)
c_v	specific heat at constant volume (J/kg K)
d	diameter of the heat pipe (m)
h	heat transfer coefficient (W/m^2 K)
k	thermal conductivity (W/m K)
K	curvature (1/m)
L	length (m)
$\dot{m}$	mass flow rate (kg/s)
p	pressure (Pa)
Q	heat flow rate (W)
R	radius of the heat pipe (m)
r	radial coordinate (m)
Re	Reynolds number
R_g	gas constant (J/kg K)
s	coordinate in meniscus (m)
t	time (s)
T	temperature (°C)
V	volume (m^3)
v_p	velocity of liquid plug (m/s)
x	axial coordinate (m)

Greek symbols

α	contact angle
δ	liquid film thickness (m)
η	coordinate normal to the inner wall (m)
μ	dynamic viscosity (kg/ms)
ρ	density (kg/m^3)
σ	surface tension (N/m)
σ_0	normal value of surface tension (N/m)

Subscripts

c	condenser
e	evaporator or environment
h	heating
l	liquid
p	plug
s	sensible
sat	saturation
v	vapor
w	wall

Wong et al. [5] presented a theoretical modeling of the PHP. The liquid film between the vapor plug and the wall is neglected, and the effect of surface tension was not taken into account. The capillary heat pipe is modeled under adiabatic conditions and there is no heat input at any part of the heat pipe. The local heat input is simulated as a sudden pressure pulse applied to a vapor plug at the evaporator section. Despite these over-simplifications, the propagation of pressure wave in the capillary heat pipe is successfully modeled. Shafii et al. [6] presented analytical models for both unlooped and looped PHPs with multiple liquid slugs and vapor plugs. Heat transfer due to exchange of sensible heat is also considered in their model and they concluded that heat transfer in both unlooped and looped PHPs is mainly due to exchange of sensible heat.

It appears that the existing theoretical model for PHPs are oversimplified. None of the existing models considered the effect of surface tension on the pressure distribution and pulsating in the heat pipe. On the other hand, none of the existing model correctly addressed the heat transfer coefficient between the working fluid (both liquid and vapor) and the tube wall. In fact, most models even neglect the existence of the liquid film between vapor plugs and the tube wall. Thermal analysis of pulsating heat pipe with open end will be presented in this paper. The effect of surface tension and heat transfer in the liquid film will be modeled, and effects of various geometric and physical parameters on the performance of pulsating heat pipe will be investigated.

2. Problem statement

A schematic of the pulsating heat pipe with one end sealed and the other end open is shown in Fig. 1. The evaporator section of the heat pipe is near the closed end, and its length is L_h. The condenser section with a length of L_c is near the open end of the heat pipe, and the adiabatic section with length L_a is located between the evaporator and condenser sections. When the evaporator is heated, the vapor pressure is increased. The liquid plug moves toward the open end since the vapor pressure, p_v, is higher than the environment pressure, p_e. As a result, the volume of the vapor slug is increased and part of the vapor slug is exposed to the cooled section of the heat pipe, where vapor is condensed to liquid. When the rate of condensation exceeds the rate of evaporation, the vapor pressure will decrease.

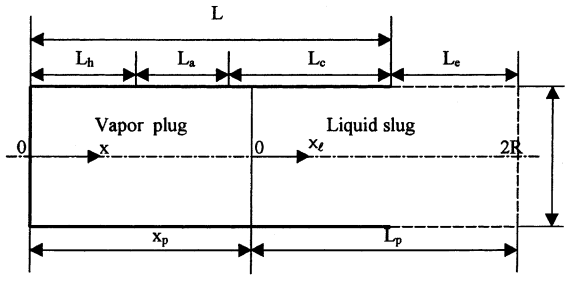

Fig. 1. Pulsating heat pipe with open end.

When the vapor pressure, p_v, is decreased to a value below the environment pressure, p_e, the liquid plug will be pushed back to the closed end. At this point, the rate of evaporation again exceeds the rate of condensation, which enables the vapor pressure increase and push the liquid plug to the open end. This process is repeated, and the oscillation of the liquid plug can be maintained in this way. As the liquid slug moves toward the open end of the pulsating heat pipe, the trailing edge of the liquid plug leaves a thin liquid film on the pipe wall [3]. The evaporation and condensation over this thin liquid film are the driving forces of pulsation flow in a PHP with open end.

In order to model heat transfer and pulsating flow in the heat pipe, the following assumptions are made:

1. The vapor is saturated and there is no temperature gradient in the vapor region.
2. Heat transport in the thin liquid films is only due to the conduction in the radial direction.
3. Inertia terms can be neglected for viscous flow in the liquid films since the Reynolds number is low.
4. Shear stress at the liquid–vapor interface is negligible.
5. The interfacial thermal resistance is negligible compared with the thermal resistance of the liquid film.

3. Heat transfer in the evaporator section

The physical model of evaporation in the evaporator section is shown in Fig. 2. The continuity equation in the coordinate system shown in Fig. 2 is

$$\int_0^{\delta} u_l \, d\eta = \frac{1}{2\pi R \rho_l}\left(\dot{m}_{l,in} - \frac{Q}{h'_{fg,e}}\right) \tag{1}$$

where Q is the rate of heat through a given cross-section due to phase change and is defined as follows:

$$Q = 2\pi R \int_0^{s} \frac{k_l(T_h - T_v)}{\delta} \, ds. \tag{2}$$

The revised latent heat of evaporation is defined as

$$h'_{fg,e} = h_{fg} + 0.68 c_{pl}(T_h - T_v) \tag{3}$$

to account for the contribution of the sensible heat.

For small Reynolds numbers (less than unity), an assumption of a fully developed laminar liquid velocity profile is valid.

$$u_l = -\frac{1}{2\mu_l}\frac{dp_l}{dx}\left(2\eta\delta - \eta^2\right). \tag{4}$$

Substituting Eq. (4) into Eq. (1), the continuity equation in the liquid film becomes

$$-\frac{dp_l}{dx} = \frac{3\mu_l}{2\pi R \rho_l \delta^3}\left(\dot{m}_{l,in} - \frac{Q}{h'_{fg,e}}\right). \tag{5}$$

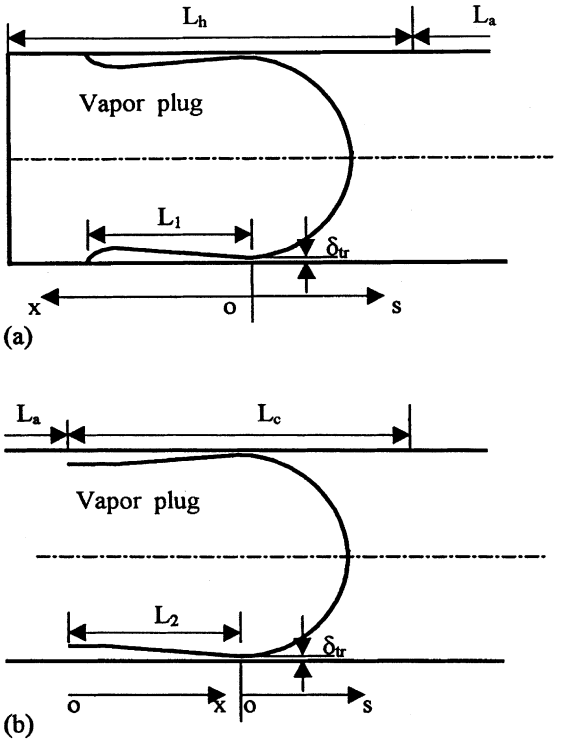

Fig. 2. Heat transfer models for the evaporator (a) and condenser (b).

The pressure in vapor and liquid phases have the following relationship:

$$p_v - p_l = \sigma K - p_d, \tag{6}$$

where the curvature is

$$K = \frac{d^2\delta}{dx^2}\left[1 + \left(\frac{d\delta}{dx}\right)^2\right]^{-3/2} + \frac{1}{R-\delta} \times \cos\left[\arctan\left(\frac{d\delta}{dx}\right)\right] \tag{7}$$

and the disjoining pressure is [7]

$$p_d = \rho_l R_g T_v \ln\left[a\left(\frac{\delta}{3.3}\right)^b\right], \tag{8}$$

where $a = 1.5336$ and $b = 0.0243$.

It is assumed that the pressure in the vapor phase is constant. By differentiating Eq. (6), we have

$$-\frac{dp_l}{dx} = \frac{d}{dx}(\sigma K - p_d). \tag{9}$$

Combining Eqs. (5) and (9), one obtains

$$\frac{d}{dx}(\sigma K - p_d) = \frac{3\mu_l}{2\pi R \rho_l \delta^3}\left(\dot{m}_{l,in} - \frac{Q}{h'_{fg,e}}\right). \tag{10}$$

The boundary conditions of Eq. (10) are:

$$\frac{\mathrm{d}\delta}{\mathrm{d}x} = 0, \quad x = 0, \tag{10a}$$

$$\frac{\mathrm{d}^2\delta}{\mathrm{d}x^2} = \begin{cases} \frac{1}{R-\delta_{\mathrm{tr}}}, & x_{\mathrm{p}} < L_{\mathrm{h}}, \\ 0, & x_{\mathrm{p}} > L_{\mathrm{h}}, \end{cases} \quad x = 0, \tag{10b}$$

$$\delta = \delta_0, \quad x = L_1, \tag{10c}$$

$$\frac{\mathrm{d}\delta}{\mathrm{d}x} = \tan\alpha, \quad x = L_1, \tag{10d}$$

where δ_0 is the non-evaporating film thickness calculated by Khrustalev and Faghri [8]

$$\delta_0 = 3.3\left\{\frac{1}{a}\exp\left[\frac{p_{\mathrm{sat}}(T_{\mathrm{h}}) - p_{\mathrm{v}}\sqrt{T_{\mathrm{h}}/T_{\mathrm{v}}} + \sigma K}{\rho_{\mathrm{l}} R_{\mathrm{g}} T_{\mathrm{h}}} + \ln\left(\frac{p_{\mathrm{v}}}{p_{\mathrm{sat}}(T_{\mathrm{h}})}\frac{T_{\mathrm{h}}}{T_{\mathrm{v}}}\right)\right]\right\}^{1/b} \tag{11}$$

and δ_{tr} in Eq. (10b) is the liquid film thickness at $x = 0$.

The liquid film thickness can be found from the numerical solution of Eq. (10). However, a simple method is proposed here. Assuming the liquid film thickness can be expressed as

$$\delta = C_0 + C_1 x + C_2 x^2 + C_3 x^3 + C_4 x^4. \tag{12}$$

Substituting Eq. (10a)–(10d) into Eq. (12), the coefficients in Eq. (12) are found to be

$$C_0 = \delta_{\mathrm{tr}}, \tag{12a}$$

$$C_1 = 0, \tag{12b}$$

$$C_2 = \begin{cases} \frac{1}{2(R-\delta_{\mathrm{tr}})}, & x_{\mathrm{p}} < L_{\mathrm{h}}, \\ 0, & x_{\mathrm{p}} > L_{\mathrm{h}}, \end{cases} \tag{12c}$$

$$C_3 = \frac{4(\delta_0 - \delta_{\mathrm{tr}}) - 2C_2 L_1^2 + L_1\tan\alpha}{L_1^3}, \tag{12d}$$

$$C_4 = \frac{-3(\delta_0 - \delta_{\mathrm{tr}}) + C_2 L_1^2 - L_1\tan\alpha}{L_1^4}. \tag{12e}$$

Integrating Eq. (10) in the interval of $(0, L_1)$, an equation about δ_{tr} is obtained

$$\rho_{\mathrm{l}} R_{\mathrm{g}} T_{\mathrm{v}} b \ln\left(\frac{\delta_{\mathrm{tr}}}{\delta_0}\right) + \sigma\frac{(\delta_0 - \delta_{\mathrm{tr}})}{(R-\delta_0)(R-\delta_{\mathrm{tr}})} - \frac{6L_1\tan\alpha - 12(\delta_0 - \delta_{\mathrm{tr}})}{L_1^2} = \frac{3\mu_{\mathrm{l}}}{2\pi R\rho_{\mathrm{l}}}\int_0^{L_1}\frac{1}{\delta^3}\left(\dot{m}_{\mathrm{l,in}} - \frac{Q}{h'_{\mathrm{fg,e}}}\right)\mathrm{d}x. \tag{13}$$

The mass flow rate of liquid at $x = 0$ is determined by an overall energy balance

$$\dot{m}_{\mathrm{l,in}} = \left.\frac{Q}{h'_{\mathrm{fg,e}}}\right|_{x=L_1}. \tag{14}$$

Eq. (13) can be solved for the liquid film thickness at the transition point, δ_{tr}. As soon as the liquid film thickness at the transition point is obtained, the liquid film thickness is calculated by Eq. (14). The total heat transfer amount for the entire thin film is then

$$Q_{\mathrm{e1}} = 2\pi R k_{\mathrm{l}}(T_{\mathrm{h}} - T_{\mathrm{v}})\int_0^{L_1}\frac{1}{\delta}\,\mathrm{d}x. \tag{15}$$

For the case of $x_{\mathrm{p}} > L_{\mathrm{h}}$, Q_{e1} is all of the heat added to the evaporator section due to evaporation. When $x_{\mathrm{p}} < L_{\mathrm{h}}$, evaporation at the meniscus must be calculated. The thickness beyond transition point is calculated by Khrustalev and Faghri [9]

$$\delta = \delta_{\mathrm{tr}} - (R - \delta_{\mathrm{tr}}) + \sqrt{(R-\delta_{\mathrm{tr}})^2 + s^2}. \tag{16}$$

The heat transfer in the meniscus region is then

$$Q_{\mathrm{e2}} = 2\pi R k_{\mathrm{l}}(T_{\mathrm{h}} - T_{\mathrm{v}})\int_0^{R-\delta_{\mathrm{tr}}}\frac{1}{\delta}\,\mathrm{d}s \tag{17}$$

and the total evaporative heat transfer for the evaporator is

$$Q_{\mathrm{evp}} = Q_{\mathrm{e1}} + Q_{\mathrm{e2}}. \tag{18}$$

4. Heat transfer in the condenser section

The analytical solution of complete condensation by Begg et al. [10] indicates that there is a point in the tube where the liquid film thickness is at its minimum. Beyond that point, the liquid film thickness increases sharply and the tube is blocked by liquid quickly. It is assumed therefore, that the liquid film in the condenser section is divided into two regions: a thin film region and a meniscus region (see Fig. 2(b)). These two regions are separated by a transition point, $x = x_{\mathrm{tr}}$, and the curvature of the liquid film in the meniscus region is assumed to be constant.

Neglecting disjoining pressure, the liquid film thickness in the thin film region of the condenser section satisfies

$$\frac{\sigma h'_{\mathrm{fg,c}}\rho_{\mathrm{l}}}{3\mu_{\mathrm{l}}}\frac{\mathrm{d}}{\mathrm{d}x}\left[\delta^3\frac{\mathrm{d}K}{\mathrm{d}x}\right] = k_{\mathrm{l}}(T_{\mathrm{v}} - T_{\mathrm{c}})\int_0^s\frac{1}{\delta}\,\mathrm{d}s, \tag{19}$$

where

$$h'_{\mathrm{fg,c}} = h_{\mathrm{fg}} + 0.68c_{\mathrm{pl}}(T_{\mathrm{v}} - T_{\mathrm{c}}). \tag{20}$$

Since the variation of the liquid film thickness in the condenser section is very small [10], the curvature of the liquid film is expressed as

$$K = \frac{\mathrm{d}^2\delta}{\mathrm{d}x^2} + \frac{1}{R-\delta}. \tag{21}$$

Substituting Eq. (21) into Eq. (19), one can obtain

$$\frac{\sigma h_{fg}\rho_l}{3\mu_l}\left[\delta^3\left(\frac{d^3\delta}{dx^3}+\frac{1}{(R-\delta)^2}\frac{d\delta}{dx}\right)\right] = k_l(T_v-T_c)\int_0^s \frac{1}{\delta}\,ds. \tag{22}$$

The boundary conditions of Eq. (22) are:

$$\frac{d\delta}{dx}=0, \quad x=0, \tag{22a}$$

$$\frac{d^2\delta}{dx^2}=0, \quad x=0, \tag{22b}$$

$$\frac{d\delta}{dx}=0, \quad x=L_2, \tag{22c}$$

$$\frac{d^2\delta}{dx^2}=\frac{1}{R-\delta_{tr}}, \quad x=L_2. \tag{22d}$$

Assuming the liquid film thickness can be expressed as

$$\delta = C_0 + C_1(x-L_2) + C_2(x-L_2)^2 + C_3(x-L_2)^3 + C_4(x-L_2)^4. \tag{23}$$

Substituting Eqs. (22a)–(22d) into Eq. (22), the liquid film thickness is

$$\delta = \delta_{tr} + \frac{1}{R-\delta_{tr}}\left[\frac{1}{2}(x-L_2)^2 + \frac{2}{3L_2}(x-L_2)^3 + \frac{1}{4L_2^2}(x-L_2)^4\right]. \tag{24}$$

At point $x=L_2$, Eq. (22) must be exactly satisfied

$$\left.\frac{\sigma h_{fg}\rho_l}{3\mu_l}\left[\delta^3\left(\frac{d^3\delta}{dx^3}+\frac{1}{(R-\delta)^2}\frac{d\delta}{dx}\right)\right]\right|_{x=L_2} = k_l(T_v-T_c)\int_0^{L_2}\frac{1}{\delta}\,ds. \tag{25}$$

Substituting Eq. (24) into Eq. (25), an equation of transition thickness is obtained

$$\frac{\sigma h_{fg}\rho_l}{3\mu_l}\left[\frac{\delta_{tr}^3}{R-\delta_{tr}}\right] = k_l(T_v-T_c)\int_0^{L_2}\frac{1}{\delta}\,ds. \tag{26}$$

Eq. (26) can be solved for liquid film thickness at the transition point, δ_{tr}. As soon as the liquid film thickness at the transition point is obtained, the liquid film thickness is calculated by Eq. (24). The total heat transfer for the entire thin film is then

$$Q_{c1} = 2\pi R k_l(T_v-T_c)\int_0^{L_2}\frac{1}{\delta}\,dx. \tag{27}$$

The liquid film thickness beyond transition point is calculated by

$$\delta = \delta_{tr} - (R-\delta_{tr}) + \sqrt{(R-\delta_{tr})^2+s^2}. \tag{28}$$

The heat transfer amount in the meniscus region is then

$$Q_{c2} = 2\pi R k_l(T_v-T_c)\int_0^{R-\delta_{tr}}\frac{1}{\delta}\,ds \tag{29}$$

and the total condensation heat transfer amount for the condenser is

$$Q_{cond} = Q_{c1} + Q_{c2}. \tag{30}$$

5. Vapor plug and liquid slug

The mass of the vapor plug increases due to evaporation at the evaporator section, and it decreases due to condensation at the condenser section. The continuity equation for the vapor is expressed as

$$\frac{dm_v}{dt} = \frac{Q_{evp}}{h'_{fg,e}} - \frac{Q_{cond}}{h'_{fg,c}}. \tag{31}$$

The energy balance for the vapor phase is

$$\frac{d(m_v c_{v,v} T_v)}{dt} = \frac{dm_v}{dt}c_{p,v}T - p_v\pi R^2\frac{dx_p}{dt}. \tag{32}$$

Eq. (32) can be rewritten as

$$m_v c_{v,v}\frac{dT_v}{dt} = \frac{dm_v}{dt}R_g T - p_v\pi R^2\frac{dx_p}{dt}. \tag{33}$$

The vapor pressure is determined using ideal gas law

$$p_v x_p \pi R^2 = m_v R_g T_v. \tag{34}$$

The momentum equation for the liquid plug is written for the entire liquid plug, both in the heat pipe and in the surroundings.

$$m_{pl}\frac{du_p}{dt} = \left(p_v - \frac{\sigma}{R_{men}} - p_e\right)\pi R^2 - 2\pi R\left[(L-x_p)\tau_p + L_e\tau_e\right]. \tag{35}$$

The effect of surface tension on the motion of the liquid plug has been included in the momentum equation. The shear stresses, τ_p and τ_e, can be calculated by using friction coefficients recommended by Dobson and Harms [3].

The evaporation and condensation heat transfer modeled in the preceding sections accounted for heat transfer from the evaporator to the condenser due to phase change. Another mechanism of heat transfer that needs to be considered is that due to sensible heat exchange between the liquid slug and the tube wall. When part of the liquid slug is located in the evaporator section, heat is added to the liquid slug in the form of sensible heat. When the liquid slug is moved to the condenser section, the sensible heat absorbed at the heating section is transferred to the wall of the condenser section. Since the liquid slug oscillates in the heat pipe at a very high frequency, the contribution of sensible heat is expected to be very important.

Since the liquid slug is assumed to be incompressible, the entire liquid slug oscillates with the same velocity, v_p. The temperature distribution in the liquid slug can be obtained by analyzing heat transfer in the liquid slug. On the moving coordinate system, x_l, that rides on the liquid slug, the problem can be described by the following equation:

$$\rho_l c_{pl} \frac{\partial T_{lm}}{\partial t} = k_l \frac{\partial^2 T_{lm}}{\partial x^2} + \frac{4h_s}{d}(T_w - T_{lm}), \tag{36}$$

where T_w is the wall temperature of the tube. It is equal to heating section temperature, T_h, for the portion of liquid located in the heating section. For the portion of liquid located in the cooling section, the wall temperature is equal to the cooling section temperature, T_c.

The initial and boundary conditions of Eq. (36) are

$$T_{lm} = T_c, \quad t = 0, \ 0 < x_l < L_c, \tag{37}$$

$$T_{lm} = T_{sat}, \quad x_l = 0, \tag{38}$$

$$T_{lm} = T_c, \quad x_l = L_c. \tag{39}$$

The liquid slug velocity, v_p, is not a constant, and therefore the Reynolds number of the liquid slug varies in a wide range that covers laminar, transition, and turbulent flow. The heat transfer coefficient in the laminar regime is obtained by using analytical solution [11]. The heat transfer coefficients in transition and turbulent regime are obtained by using empirical correlations in the literature [6].

The heat transferred into the liquid slug due to single phase convection is

$$Q_{hs} = \begin{cases} \int_0^{L_h - x_p} \pi \, dh_e (T_h - T_{lm}) \, dx_l, & x_p < L_h, \\ 0, & x_p \geqslant L_h. \end{cases} \tag{40}$$

The heat transferred from the liquid slug to the tube wall is

$$Q_{cs} = \int_0^{L_c} \pi \, dh_e (T_{lm} - T_c) \, dx_l. \tag{41}$$

The FORTRAN code has been written based on the above model. The code include four major parts: (1) liquid slug and vapor plug motion, (2) evaporation, (3) condensation, and sensible heat transfer in the liquid slug. An explicit finite difference scheme was employed to solve the governing equations of the vapor plug and the liquid slug. An implicit scheme with non-uniform grid [12] was employed to solve transient heat transfer in the liquid slug. The time step independent solution of the problem can be obtained when time step is 0.0001 s, which is then used in all numerical simulations in this paper.

6. Results and discussion

The present model is used to simulate the pulsating heat pipe with the following parameters: $L_h = 0.15$ m, $L_a = 0$, $L_c = 0.2$ m, $T_h = 120$ °C, and $T_c = 20$ °C. The variations of liquid slug location, x_p, vapor pressure, p_v, and the vapor temperature, T_v, with time are shown in Fig. 3. It can be seen that the oscillating vapor pressure due to thin film evaporation and condensation makes the operation of pulsating heat pipe possible. Steady oscillation is established after $t = 0.5$ s. The variation of average mean temperature of the liquid slug is shown in Fig. 4. It can be seen that steady oscillation of average mean temperature is not established until $t = 5$ s, which is much longer that the time to achieve steady oscillation of PHP.

The heat transfer due to latent heat and sensible heat is shown in Fig. 5. It can be seen that the contribution of sensible heat on the total heat transfer amount is significantly larger that of latent heat. The average heat

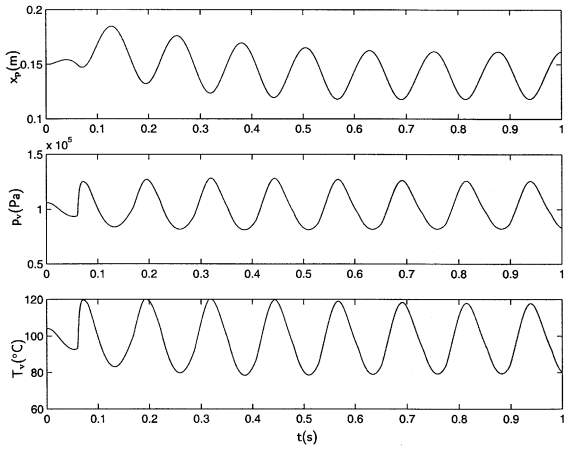

Fig. 3. Slug location, vapor pressure and temperature by present model.

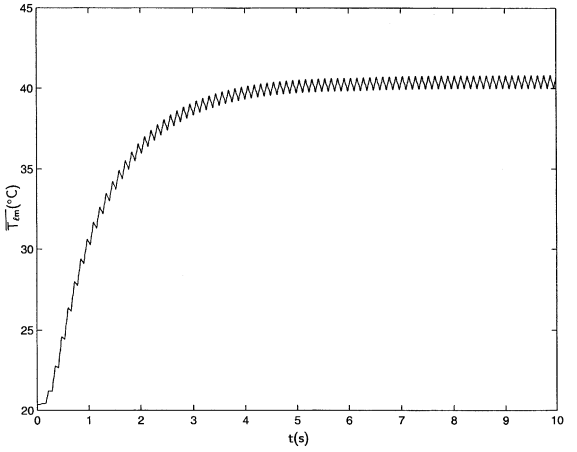

Fig. 4. Average mean temperature of liquid slug.

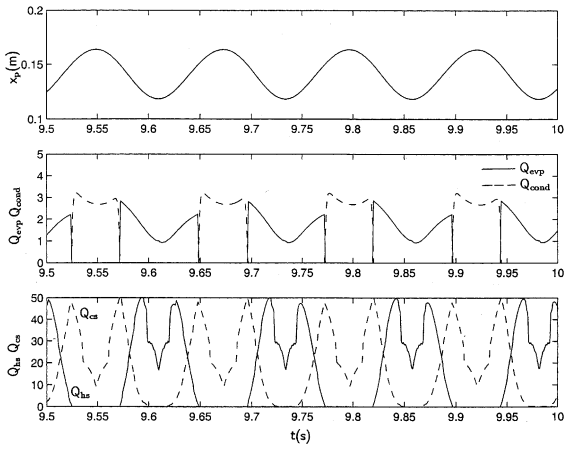

Fig. 5. Contribution of latent and sensible heat on heat transfer in PHPs.

transferred due to evaporation and condensation for one period of the heat pipe operation is 1.11 W. The average sensible heat transfer for the same time period is 18.05 W, which represents an overall contribution of 90% (see Table 1). It can be concluded that heat transfer in a PHP is mainly due to the exchange of sensible heat. The role of the evaporation and condensation on the operation of PHPs is mainly on oscillation of liquid slug and the contribution of latent heat on the overall heat transfer is not significant. The effect of sensible heat on film evaporation and condensation are considered by using revised latent heat defined in Eqs. (3) and (20). Fig. 6 shows the effect of sensible heat correction on the performance of PHP with one open end. It can be seen that the sensible heat correction has very little effect on the overall performance.

Another improvement of the present model is that the effect of surface tension on the momentum balance of liquid is taken into account by considering the capillary pressure $-\sigma/(R-\delta_{tr})$ as indicated in Eq. (35). Fig. 7 shows the effect of capillary pressure on the location of the liquid slug, vapor pressure and vapor temperature of the pulsating heat pipe. It is clearly seen that the effect of capillary pressure on the performance of the pulsating heat pipe is negligible. On the other hand, the surface tension is very important for the thin film thickness in both the evaporator and condenser sections. The effect of surface tension on the performance of the pulsating heat pipe is shown in Fig. 8. In addition to the results for the surface tension at its normal value, σ_0, the results with doubled and halved surface tension are also shown in Fig. 8 for purpose of comparison. It can be seen from Fig. 8(a) that the curves of x_p shifted to the right with decreased surface tension and to the left with increased surface tension. However, the frequency and amplitude of the oscillation is almost the same after steady oscillation is established. Fig. 8(b) shows the effect of surface tension on vapor pressure. It is seen that the vapor pressure slightly decreases with increasing surface tension. The effect of surface tension on the vapor temperature is shown in Fig. 8(c). It can be seen that the vapor temperature decreases with increasing surface tension. Fig. 9 shows the liquid plug location, vapor pressure and temperature for the PHP with an initial liquid plug location of $x_{p0} = 0.1$ m. It is seen that pulsating flow can be established when the liquid slug is initially located in the evaporator section. The frequency and amplitude of oscillation for $x_{p0} = 0.1$ m is same as that for $x_{p0} = 0.15$ m. The phase differences of oscillation for $x_{p0} = 0.1$ m and $x_{p0} = 0.15$ m is about π.

The effect of diameter on performance of PHPs is shown in Fig. 10. It can be seen that the curves of x_p, p_v and T_v shifted to left with decreasing pipe diameter. In addition, the amplitude of oscillation decreases with decreasing diameter. The effect of pipe diameter, however on the frequency of oscillation is insignificant. The effect of the diameter on vapor pressure is shown in Fig. 10(b). The amplitude of the pressure curve decreases with decreasing diameter. The amplitude of the temperature oscillation is increased with decreasing tube diameter.

The effect of evaporator section temperature on the performance is shown in Fig. 11. It can be seen that steady oscillation can be established and maintained when the wall temperature of heating section is decreased to 110 °C. The amplitudes of oscillation for

Table 1
Total heat transport rate and contribution of latent and sensible heat transfer

Cases	Latent heat	$-\sigma/(R-\delta_{tr})$ in Eq. (34)	σ (N/m)	d (mm)	T_h (°C)	$\overline{Q_{evp}}$ (W)	$\overline{Q_{h,s}}$ (W)	$\overline{Q_t}$ (W)	$\overline{Q_{h,s}}/\overline{Q_t}$ (%)
1	h'_{fg}	Yes	σ_0	3.34	120	1.11	18.05	19.16	94.2
2	h_{fg}	Yes	σ_0	3.34	120	1.14	18.83	19.97	94.3
3	h'_{fg}	No	σ_0	3.34	120	1.11	12.18	13.30	94.3
4	h'_{fg}	Yes	$2\sigma_0$	3.34	120	1.23	19.71	20.93	94.1
5	h'_{fg}	Yes	$\sigma_0/2$	3.34	120	1.01	16.55	17.56	94.3
6	h'_{fg}	Yes	σ_0	3.34	110	0.97	14.05	15.02	93.6
7	h'_{fg}	Yes	σ_0	1.67	120	0.47	6.13	6.60	92.9

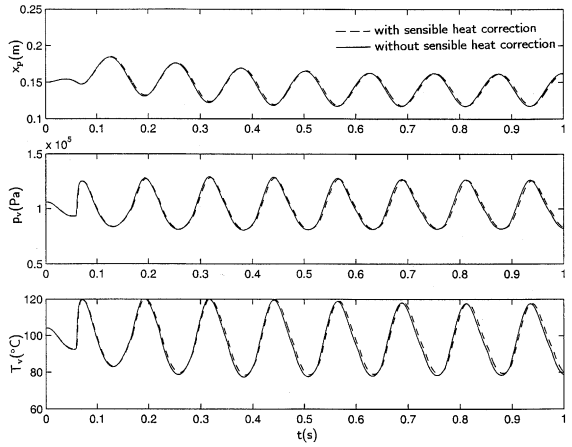

Fig. 6. Effect of sensible heat correction on PHP performance.

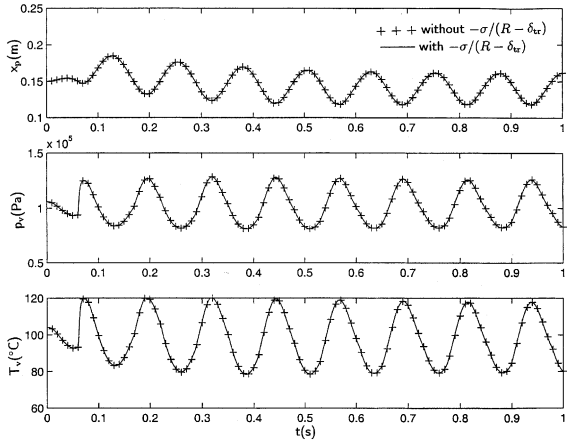

Fig. 7. Effect of the capillary pressure in liquid momentum equation on performance of PHP.

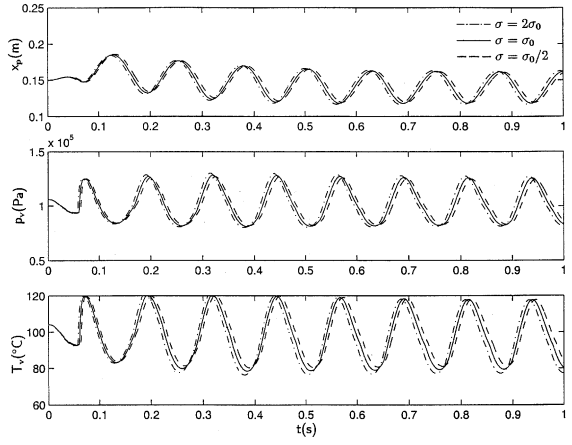

Fig. 8. Effect of surface tension on PHP performance.

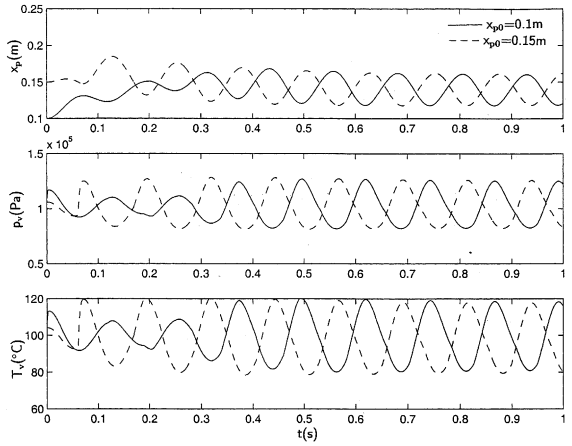

Fig. 9. Effect of initial slug location on PHP performance.

liquid plug location, vapor pressure, and vapor temperature are decreased when the evaporator section temperature is decreased. The frequency of oscillation, however is almost not changed after steady oscillation has been established. Fig. 12 shows the effect of the evaporator length on PHP performance. The length of the evaporator section is increased to 0.2 m, but the initial plug location remains at $x_{p0} = 0.15$ m. It can be seen from Fig. 12(a) that the steady oscillation is established after $t = 0.5$ s. Compared with the results of $x_{p0} = 0.15$ m, the average value and amplitude of the oscillation of x_p is increased since the volume of the vapor is larger.

The total heat transport rate of a PHP with open end, Q_t, which includes the contribution of both latent and sensible heat, is a very important parameter for a PHP. For the cases investigated in the parametric study, the total heat transport rate as well as the contribution of latent and sensible heat transfer are listed in Table 1.

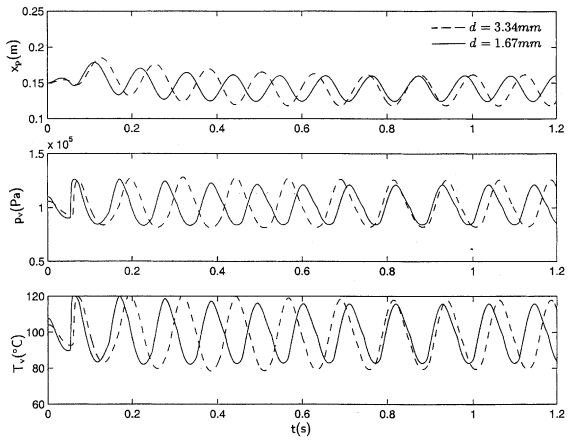

Fig. 10. Effect of diameter on PHP performance.

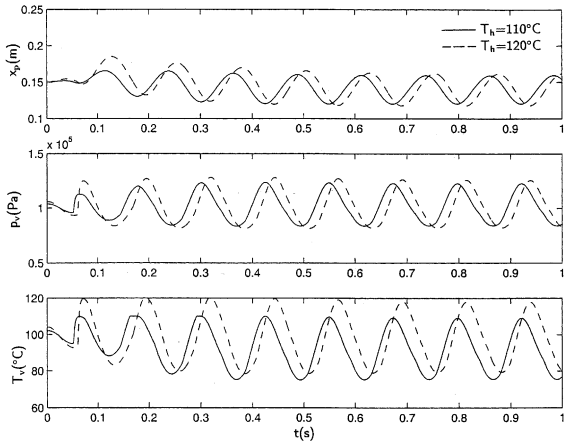

Fig. 11. Effect of evaporator temperature on PHP performance.

The evaporative and sensible heat transfer rate listed in Table 1 are the average heat transfer for one period after steady oscillation is established. The maximum difference between average condensation heat transfer rate, $\overline{Q_{\mathrm{cond}}}$, which are not listed in Table 1, and the average evaporative heat transfer rate, $\overline{Q_{\mathrm{evp}}}$, is less than 2%. The average heat transfer rate to the condenser section due to sensible heat, $\overline{Q_{\mathrm{c,s}}}$, and that from the evaporator section, $\overline{Q_{\mathrm{h,s}}}$, agreed very well (maximum difference less than 1%) which means that the PHP is operated at a steady oscillation condition.

It can be seen from Table 1 that, for most cases, the contribution of sensible heat on the total heat transport rate is over 90%, which is significantly larger that of latent heat for all cases investigated. The total heat transport rate, $\overline{Q_{\mathrm{t}}}$, is increased by 10% if the latent heat is not corrected by Eqs. (3) and (20). The effect of capillary pressure term $-\sigma/(R-\delta_{\mathrm{tr}})$ in Eq. (35) on the overall heat transfer rate is negligible. The overall heat transport rate increases with increasing surface tension. The overall heat transfer rate is decreased with decreasing the evaporator section temperature. When the diameter of the PHP is reduced by half, the overall heat transfer decreased from 19.16 W all the way to 6.60 W since both cross-sectional area and the area for heat transfer is significantly reduced.

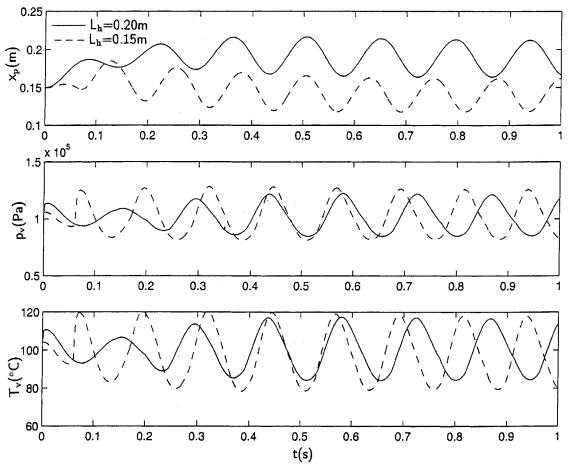

Fig. 12. Effect of heating section length on PHP performance ($L_{\mathrm{h}} = 0.2$ m, $x_{\mathrm{p0}} = 0.15$ m).

7. Conclusion

Heat transfer models in the evaporator and condenser sections of a pulsating heat pipe with one open end are developed by analyzing thin film evaporation and condensation. Heat transfer in a PHP is due mainly to the exchange of sensible heat. The role of evaporation and condensation on the operation of PHPs is mainly on the oscillation of liquid slugs and the contribution of latent heat on the overall heat transfer is not significant. The effect of capillary pressure on the momentum equation of liquid slug is studied and the results show that its effect is negligible. The frequency and amplitude of the oscillation is almost unaffected by surface tension after steady oscillation has been established. The amplitude of oscillation is decreased with decrease of diameter of the pulsating heat pipe. The amplitude of oscillation is decreased when the wall temperature of the heating section is decreased, but the frequency of oscillation is almost unchanged.

Acknowledgements

Funding for this work was provided by NASA Grant NAG3-1870 and NSF Grant CTS 9706706.

References

[1] H. Akachi, Looped Capillary Heat Pipe, Japanese Patent, No. Hei6-97147, 1994.
[2] W.H. Lee, H.S. Jung, J.H. Kim, J.S. Kim, Flow visualization of oscillating capillary tube heat pipe, in: Proceedings of the 11th International Heat Pipe Conference, Tokyo, Japan, 1999, pp. 131–136.
[3] R.T. Dobson, T.M. Harms, Lumped parameter analysis of closed and open oscillatory heat pipes, in: Proceedings of the 11th International Heat Pipe Conference, Tokyo, Japan, 1999, pp. 137–142.
[4] M. Hosoda, S. Nishio, R. Shirakashi, Meandering closed-loop heat-transport tube (propagation phenomena of vapor plug), in: Proceedings of the 5th ASME/JSME Joint

Thermal Engineering Conference, March 15–19, San Diego, CA, 1999.
[5] T.N. Wong, B.Y. Tong, S.M. Lim, K.T. Ooi, Theoretical modeling of pulsating heat pipe, in: Proceedings of the 11th International Heat Pipe Conference, Tokyo, Japan, 1999.
[6] M.B. Shafii, A. Faghri, Y. Zhang, Thermal modeling of unlooped and looped pulsating heat pipes, ASME J. Heat Transfer 123 (2001).
[7] A. Faghri, Heat Pipe Science and Technology, Taylor & Francis, Washington, DC, 1995.
[8] D. Khrustalev, A. Faghri, Heat transfer during evaporation on capillary-grooved structures of heat pipes, ASME J. Heat Transfer 117 (1995) 740–747.
[9] D. Khrustalev, A. Faghri, Thick-film phenomenon in high-heat-flux evaporation from cylindrical pores, ASME J. Heat Transfer 119 (1997) 272–278.
[10] E. Begg, D. Khrustalev, A. Faghri, Complete condensation of forced convection two-phase flow in a miniature tube, ASME J. Heat Transfer 121 (1999) 904–915.
[11] A. Bejan, Convection Heat Trasnsfer, second ed., Wiley, New York, 1995.
[12] S.V. Patankar, Numerical Heat Transfer and Fluid Flow, Hemisphere, New York, 1980.